

COMPARATIVE ANALYSIS OF THE AVERAGE MULTIPLICITIES OF CHARGED SECONDARY HADRONS, PRODUCED IN ELECTRON-POSITRON, PROTON-PROTON (ANTIPROTON) AND PROTON-NUCLEUS COLLISIONS

L. Akhobadze, V. Garsevanishvili, T. Jalagania, Yu. Tevzadze,
G. Vanishvili

Accepted for publication February, 2006

ABSTRACT. The $\langle n_{\text{ch}}(\mathbf{s}) \rangle \cong \langle n(\mathbf{s}) \rangle$ dependence on energy of the average multiplicity of charged secondary hadrons produced in electron-positron, proton-proton (antiproton) and proton-nucleus collisions is analysed on the basis of following models: Statistical model, Field-Feynman model, Cluster model and Lund model and parton-hadrons local duality model or Perturbative quantum chromodynamics.

I. INTRODUCTION

Characteristics of secondaries in hh -hadron-hadron, hA_t -hadron-nucleus and e^+e^- -electron-positron collisions are studied for many decades in cosmic rays and at the accelerators as well. For the analysis of experimental data up to 60-ies of the XX century (prequark epoch) different theoretical models have been developed (classical and quantum). These models described the main experimental regularities of soft processes – weak growth of the interaction cross section and multiplicity with increasing energy, restriction of the transverse momenta of secondaries, etc.

These models can be divided conventionally into two groups: statistical and multiperipheral. The first group starts from the notions of classical physics, taking into account some quantum effects – it is assumed initial hadrons form an excited, so called compound-system, which decays according to the laws of statistics [1,2].

The second group of models is based on quantum field theory. The production process is considered as a result of creation of many excited centers (resonances, clusters). One of the representatives of this group

is a multiperipheral model, and its development is connected with the parton description of multiparticle processes. The existence of different approaches shows that at present we are far from the construction of the unique picture of soft processes. But the description of some significant regularities of inclusive processes in terms of these models allows (in some sense) to construct fragments of this picture. The successes of these models should be taken into account in the development of the quark-parton interaction picture.

The experimental observation of quarks and gluons stimulated the creation of new model for hadronic interactions-quark model have been developed intensively, which have been applied for the explanation of some physical regularities [3,4,5]. In these studies two different areas of the application of quark-parton models are distinguished: a) the soft collision region-small momentum transfer (less than 1GeV/c, large distances, $\sim 1F$), in which the model is of the phenomenological nature, b) hard collisions region – large momentum transfer ($>1\text{GeV}/c$) and small distances (less than 0.1 F), where the perturbative QCD can be applied. QCD successfully describes the interaction of colored partons (quarks and gluons) at small distances due to the remarkable property of this theory (asymptotic freedom). At large distances for the description of the hadronization of quarks phenomenological models are used. On the other hand, it is clear that physics of hard and soft processes is unique and it is necessary to consider them together for the construction of the strong interaction theory. It should be noted that in all quark parton models the main problem is the quark (parton, cluster) hadronization.

In the present paper the $\langle n_{ch}(s) \rangle \cong \langle n(s) \rangle$ dependence on energy of the average multiplicity of charged secondary hadrons produced in electron-positron, proton-proton (antiproton) and proton-nucleus collisions is analysed on the basis of following models: SM(1) - Statistical model, FFM(2) - Field-Feynman model, CLM and LM(3) - Cluster model and Lund model and parton-hadrons local duality model or PQCD(4) - Perturbative quantum chromo dynamics (4) [1,2].

The above mentioned models give for the $\langle n_{ch}(s) \rangle \cong \langle n(s) \rangle$ dependence the following relations:

$$\langle n_{\text{ch}}(s) \rangle \cong \langle n(s) \rangle \rightarrow \begin{cases} a s^\beta & SM, & (1) \\ a + b \ln s & FFM, & (2) \\ a + b \ln s + c(\ln^2 s) & CLM(LM), & (3) \\ a + b \exp(c_1 \sqrt{\ln s}) & PQCD, & (4) \end{cases}$$

where s is the square of the total energy in the c. m. s., a , β , b , c are free parameters, which are extracted from the experiment; parameter c_1 is calculated according to the formula [1,2]:

$$c_1 = \left(\frac{72}{33 - 2N_q} \right)^{1/2}, \quad (5)$$

where N_q is the number of quark flavours, c_1 can be considered as a free parameter as well.

The problem of quark (parton, cluster) hadronization is treated in different ways in different models. The model description of quarks is given either by PQCD or by the phenomenological approach.

In CLM(3) – cluster models hadronization is described without introduction of fragmentation function and restriction of parton transverse momenta. The first stage of the hard process-production of parton shower, is considered in the framework of the QCD. Due to the long distance colour forces the quarks and antiquarks form colorless clusters and after words hadronization of clusters is realized.

Hadronization of quarks in the FFM(2) in similar to the production of hadrons in the parton model. Hadrons are produced through the consecutive and independent decays:

$$q_a \rightarrow q_b + M, \quad (6)$$

where initial quark (q_a) is fragmented into the meson M and the new quark (q_b), then q_b decays again according to the scheme (6). In the LM(3)-Lund model, the evolution of quark-antiquark systems is

considered taking into account the character of colour forces between quarks.

In the LM(3) it is possible to take into account the conservation of energy and quantum numbers. In this sense LM(3) is more adequate, than the FFM(2).

In the PQCD the parameter c_I is given by the relation (5) and takes the values:

$$c_I = \begin{cases} 1.63 & N_q = 3 \\ 1.70 & N_q = 4 \\ 1.77 & N_q = 5 \end{cases} \quad (7)$$

2. ANALYSIS OF EXPERIMENTAL DATA

The $\langle n(s) \rangle$ dependence on energy of the average multiplicity of charged secondary hadrons in e^+e^- , pp^* and pA_t -collisions is analysed on the basis of above mentioned models (See expressions (1), (2), (3), (4)).

pTa interaction is analysed to study the role of the heavy target nucleus. The results of the analysis are compared to each other in the same energy intervals, if possible. The experimental data are taken from the current literature [1-10].

The SM(1) describes rather well the data for e^+e^- collisions, especially for high energy intervals ((14-130), (14-91), (10-130), (10 - 200) GeV) (see Tables 1 and 7).

The value of the parameter β is located in the narrow interval $(0.20 \pm 0.01 \div 0.28 \pm 0.01)$. In high energy intervals the parameter β is slightly decreased to the value 0.20 ± 0.01 . The inclusion of low energy data (low average multiplicities) causes the increase of the parameter β to the value 0.28 ± 0.01 (Table 9). So the role of neutral

* In the following we use the notation pp for both pp and proton-antiproton-collisions.

particles in $\langle n(s) \rangle$ is increased with increasing energy. (We will return to this point later).

The description of $\langle n(s) \rangle$ dependence by the SM(1) for $pp -$ collisions is worse, than in e^+e^- collisions. However the qualitative picture is the same. Namely, in low energy intervals ($2 \leq \sqrt{s} \leq 22$) GeV the tendency of increasing of β (0.32 ± 0.01 , Table 9) is observed. The inclusion of high energy data causes the decreasing of β to the value 0.22 ± 0.01 (Table 1. ($10 \leq \sqrt{s} \leq 200$) GeV).

The fact, that the multiplicity in e^+e^- interactions is always more than in pp -collisions (of course at fixed energy) can be explained by the baryon number conservation and by leading particles, which take the significant part of the initial energy.

Table 1.

The values of the parameters a, b, β, c and c_1 in the approximation of the $\langle n(\mathbf{s}) \rangle$ dependence by the expressions (1),(2), (3), (4)

e^+e^- -collisions ($1.5 \leq \sqrt{s} \leq 200$)GeV

Formula	a	$b(\beta)$	c	χ^2/N
SM(1)	2.56 ± 0.07	0.23 ± 0.01		75/48
FFM(2)	-1.77 ± 0.14	2.39 ± 0.03		540/48
CLM(LM)(3)	2.81 ± 0.25	-0.07 ± 0.11	0.23 ± 0.01	18/48
PQCD(4)	1.24 ± 0.19	0.37 ± 0.04	1.31 ± 0.03	30/48

e^+e^- -collisions ($10 \leq \sqrt{s} \leq 200$)GeV

SM(1)	3.31 ± 0.29	0.20 ± 0.01		10/31
FFM(2)	-11.11 ± 0.67	3.55 ± 0.09		36/31
PQCD(4)	-0.21 ± 0.95	0.65 ± 0.14	1.15 ± 0.06	8/31

pp -collisions ($10 \leq \sqrt{s} \leq 200$) GeV

SM(1)	2.06 ± 0.11	0.22 ± 0.01		28/11
FFM(2)	-5.17 ± 0.42	2.17 ± 0.07		36/11
PQCD(4)	-1.15 ± 0.87	0.64 ± 0.19	1.07 ± 0.08	19/11

The experimental fact of the significant difference of average multiplicity in e^+e^- and pp -collisions is reflected in the inequality of parameters a : $a_{e^+e^-} = 3.31 \pm 0.29$; $a_{pp(p)} = 2.06 \pm 0.11$ (Table 1).

The cluster model and the Lund model – CLM(LM) describe well data for pp and especially for e^+e^- -collisions. Simplest quark-parton models predict the logarithmic dependence of $\langle n(s) \rangle$, i. e. $\langle n(s) \rangle \sim \ln s$. However, the analysis of data shows, that $\langle n(s) \rangle$ increases faster than $\ln s$ and the term $\ln^2 s$ is decisive. For instance, in e^+e^- -collisions in the intervals including low energy data (Tables 2, 3, 4, 6) the value of coefficient c (before $\ln^2 s$) is equal to 0.23 ± 0.01 . High energy data give for c the value 0.34 ± 0.02 (Table 7).

In pp -collisions the value of the coefficient c is always less than in e^+e^- -collisions and equals to 0.14 ± 0.01 . On the other hand, it is known, that the average multiplicity of hadrons in jets is increased $\sim \ln^2 s$.

One can conclude, that in e^+e^- -collisions the jet structure is more pronounced, than in pp - and in pA_t -proton-nucleus collisions. This is confirmed also from different points of view and experiments [1].

It is interesting to note, that in e^+e^- -collisions the coefficients b and c have different signs ($b < 0$), but in pp -collisions they have the same sign.

Table 2.

The values of parameters a, b, β, c, c_l in the approximation of the $\langle n(\mathbf{s}) \rangle$ dependence by formulae (1), (2), (3), (4)

$$(3 \leq \sqrt{s} \leq 200) \text{ GeV}, e^+e^-$$

Formula	a	$b(\beta)$	$c(c_l)$	χ^2/N
SM(1)	2.60±0.08	0.23±0.01		69/45
FFM(2)	-3.85±0.18	2.69±0.04		250/45
CLM(LM)(3)	2.72±0.49	-0.04±0.19	0.23±0.01	17/45
PQCD(4)	0.28±0.24	0.54±0.05	1.21±0.03	21/45

$$(3 \leq \sqrt{s} \leq 200) \text{ GeV}, pp$$

SM(1)	1.52±0.02	0.27±0.01		174/22
FFM(2)	-1.20±0.06	1.48±0.02		270/22
CLM(LM)(3)	1.17±0.15	0.28±0.07	0.14±0.01	30/22
PQCD(4)	0.024±0.087	0.41±0.02	1.20±0.02	30/22

$$(3 \leq \sqrt{s} \leq 30) \text{ GeV}, e^+e^-$$

SM(1)	2.06±0.31	0.27±0.01		13/17
FFM(2)	-1.12±0.30	1.93±0.08		32/17
CLM(LM)(3)	3.10±0.80	-0.24±0.46	0.25±0.02	10/17
PQCD(4)	1.50±0.35	0.24±0.07	1.48±0.009	12/17

$$(3 \leq \sqrt{s} \leq 30) \text{ GeV}, pp$$

SM(1)	1.38±0.02	0.29±0.01		50/16
FFM(2)	-0.99±0.07	1.42±0.02		146/16
CLM(LM)(3)	1.18±0.15	0.27±0.02	0.14±0.01	17/16
PQCD(4)	0.22±0.08	0.33±0.02	1.28±0.02	18/16

Table 3.

The values of parameters a , b , β , c , c_1 in the approximation of the $\langle n(s) \rangle$ dependence by formulae (1), (2), (3), (4)

$(3 \leq \sqrt{s} \leq 130)$ GeV, e^+e^- -collisions

Formula	a	$b(\beta)$	$c(c_1)$	χ^2/N_p
SM(1)	2.32±0.09	0.25±0.01		28/30
FFM(2)	-2.75±0.20	2.41±0.03		110/30
CLM(LM)(3)	2.91±0.62	-0.13±0.27	0.23±0.02	14/30
PQCD(4)	0.88±0.47	0.39±0.10	1.31±0.08	15/30

$(3 \leq \sqrt{s} \leq 130)$ GeV, pp

SM(1)	1.48±0.01	0.27±0.01		143/21
FFM(2)	-1.13±0.06	1.46±0.02		190/21
CLM(LM)(3)	1.02±0.17	0.36±0.08	0.13±0.01	24/21
PQCD(4)	-0.19±0.09	0.46±0.03	1.16±0.02	28/21

In e^+e^- -collisions (in high energy intervals, Table 7) together with the growth of the influence of $\ln^2 s$ -term, the role at the $\ln s$ -term also increases. The parameter b reaches the value ~ 2 (with minus sign). Thus, in e^+e^- -collisions the growth of the influence of the $\ln^2 s$ -term causes the growth of the influence of the logarithmic term, as well.

In pp -collisions the situation is opposite: weak growth of the influence of the $\ln^2 s$ -term (small growth of the parameter c) causes the significant decrease of the logarithmic term (significant decrease of the coefficient b) (Table 5). And vice versa: some decreases of the value the parameter c , causes the significant growth of the parameter b (Tables 2, 3).

The PQCD describes well the $\langle n(s) \rangle$ dependence for e^+e^- -collisions and for pp -collisions as well. However, values of the parameter c_I extracted from the approximation do not correspond to values obtained from the formula (7), for instance the maximal value of the parameter $c_I=1.54\pm 0.07$ (Table 6, e^+e^- , $(1.5 \leq \sqrt{s} \leq 30)$ GeV).

If proceed from table values (7) and do not consider c_I as a free parameter, the good description is obtained only for e^+e^- -collisions, when $c_I = 1.77$ ($N_q = 5$), $(14 \leq \sqrt{s} \leq 200)$ GeV. (Table 8)

We studied also the $\langle n(s) \rangle$ -dependence for pTa -collisions and results were compared with the results for e^+e^- and pp -collisions in the interval $(2 \leq \sqrt{s} \leq 22)$ GeV, (Table 9).

In e^+e^- and pp -collisions $\langle n(s) \rangle$ dependence (according to SM (1)) increased equally fast ($\beta \approx 0.30$).

In pTa -collisions more rapid growth is observed ($\beta \approx 0.45$). In the beginning (up to $\sqrt{s} \leq 5$ GeV) a most rapid growth is observed and further the growth is significantly slower, β is approximately the same as in e^+e^- and pp -collisions (Fig.1).

Table 4.

Values of parameters a , b , β , c , c_I in the approximation of the $\langle n(s) \rangle$ dependence by formulae (1), (2), (3), (4)

$(1.5 \leq \sqrt{s} \leq 91)$ GeV, e^+e^- -collisions

Formula	a	$b(\beta)$	$c(c_I)$	χ^2/N_p
SM(1)	2.28 ± 0.08	0.25 ± 0.01		25/31
FFM(2)	-0.73 ± 0.15	2.05 ± 0.03		240/31
CLM(LM)(3)	2.83 ± 0.28	-0.09 ± 0.14	0.23 ± 0.01	13/31
PQCD(4)	1.72 ± 0.22	0.25 ± 0.04	1.45 ± 0.05	19/31

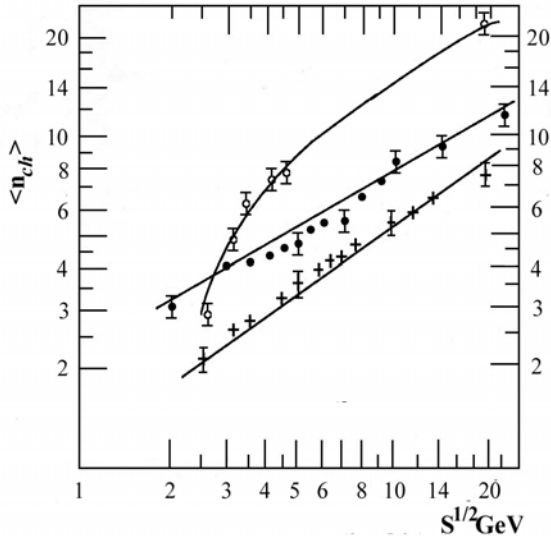


Fig.1. $\langle n(s) \rangle$ dependence for $pp(+)$, e^+e^- (\bullet) and $pTa(\circ)$ - collisions. Solid line – approximation by CLM(LM) (formula (3))

$$(1.5 \leq \sqrt{s} \leq 130) \text{ GeV}, e^+e^-$$

SM(1)	2.31 ± 0.07	0.25 ± 0.01		28/33
FFM(2)	-0.70 ± 0.15	2603 ± 0.30		250/33
CLM(LM)(3)	2.89 ± 0.27	-0.08 ± 0.14	0.22 ± 0.01	14/33
PQCD(4)	1.65 ± 0.21	0.26 ± 0.04	1.43 ± 0.05	15/33

Table 5.

Values of parameters a, b, β, c, c_I in the approximation of the $\langle n(\mathbf{s}) \rangle$ dependence by formulae (1), (2), (3), (4)
 $(3 \leq \sqrt{s} \leq 900) \text{ GeV}, pp$

Formula	a	$b(\beta)$	$c(c_I)$	χ^2/N_p
SM(1)	1.70±0.03	0.24±0.01		437/23
FFM(2)	-2.57±0.16	1.96±0.03		227/23
CLM(LM)(3)	1.85±0.33	-0.09±0.14	0.17±0.01	10/23
PQCD(4)	0.06±0.32	0.41±0.07	1.19±0.05	9/23

Table 6.

Values of parameters a, b, β, c, c_I in the approximation of the $\langle n(\mathbf{s}) \rangle$ dependence by formulae (1), (2), (3), (4)
 $(3 \leq \sqrt{s} \leq 60) \text{ GeV}, e^+e^-$

Formula	a	$b(\beta)$	$c(c_I)$	χ^2/N
SM(1)	2.21±0.09	0.26±0.01		17/25
FFM(2)	-2.32±0.22	2.29±0.05		71/25
CLM(LM)(3)	2.91±0.64	-0.13±0.25	0.24±0.02	12/25
PQCD(4)	1.16±0.26	0.32±0.05	1.37±0.05	14/25

$(3 \leq \sqrt{s} \leq 60) \text{ GeV}, pp$

SM(1)	1.44±0.02	0.27±0.01		93/20
FFM(2)	1.09±0.06	1.45±0.02		141/20
CLM(LM)(3)	1.07±0.17	0.33±0.08	0.13±0.01	23/20
PQCD(4)	0.018±0.085	0.41±0.02	1.20±0.02	25/20

$(1.5 \leq \sqrt{s} \leq 30) \text{ GeV}, e^+e^-$

SM(1)	2.21±0.08	0.26±0.01		17/23
FFM(2)	-0.09±0.16	1.81±0.04		149/23
CLM(LM)(3)	2.84±0.30	-0.09±0.17	0.23±0.02	12/23
PQCD(4)	1.93±0.28	0.20±0.04	1.54±0.006	16/23

Table 7.

Values of parameters a, b, β, c, c_1 in the approximation of the $\langle n(s) \rangle$ dependence by formulae (1), (2), (3), (4)

$(14 \leq \sqrt{s} \leq 91) \text{ GeV}, e^+e^-$

Formula	a	$b(\beta)$	$c(c_1)$	χ^2/N
SM(1)	2.94±0.44	0.22±0.02		3/14
FFM(2)	-7.28±1.06	3.01±0.14		9/14
CLM(LM)(3)	7.92±1.15	-1.40±0.28	0.31±0.02	2/14
PQCG(4)	1.00±0.91	0.45±0.11	1.26±0.07	3/14

$(14 \leq \sqrt{s} \leq 130) \text{ GeV}, e^+e^-$

SM(1)	2.94±0.43	0.22±0.02		3/16
FFM(2)	-8.33±0.97	3.16±0.13		16/16
CLM(LM)(3)	9.46±1.12	-1.86±0.28	0.34±0.02	3/16
PQCD(4)	2.01±0.90	0.30±0.15	1.38±0.16	3/16

* In the interval $(3 \leq \sqrt{s} \leq 50) \text{ GeV}$ the same results are obtained as in the interval $(3 \div 60) \text{ GeV}$.

$$(10 \leq \sqrt{s} \leq 130) \text{ GeV}, e^+e^-$$

SM(1)	2.97±0.45	0.22±0.02		3/18
FFM(2)	-6.38±0.72	2.91±0.07		26/18
CLM(LM)(3)	9.20±0.99	-1.80±0.28	0.34±0.02	3/18
PQCD(4)	2.95±0.61	0.21±0.04	1.47±0.06	3/18

The reason of the rapid growth of the multiplicity in the beginning (up to $\sqrt{s} \approx 5$ GeV) seems to be in the significant absorption of slow secondaries in the heavy target nucleus Ta [5]. In higher interval the intranuclear scattering (cascading) is more significant, than absorption.

Table 8.

Values of parameters a and b in the approximation of the $\langle n(s) \rangle$ dependence by formula (4) (PQCD) for e^+e^- -collisions (fixed values of c_l (formula (5))

a	b	$c_l \text{ fix}$	Energy range (\sqrt{s})GeV	χ^2/N
2.73±0.11	0.132±0.001	1.63±($N_q=3$)	1.5÷200	85/48
3.28±0.14	0.102±0.001	1.70($N_q=4$)	4÷200	93/43
5.89±0.24	0.070±0.001	1.77($N_q=5$)	14÷200	16/31

At more higher energies (>10 GeV) the role of neutral particles in the total multiplicity increases and one observes a less rapid growth of the multiplicity of charged secondaries (confirmed by experimental data) [11].

It is interesting to be mentioned, that in contrast to pp and especially to e^+e^- -collision, in the analysis of $\langle n(s) \rangle$ -dependence in pTa -collisions in the framework of CLM (LM) (3) the logarithmic term dominates and the parameter c is practically equal to zero. The

reason seems to be in following: in this energy range in pTa -collision the jet structure is less pronounced, than in e^+e^- and pp -collisions. (Table 9, Fig. 1).

Table 9.

Values of coefficients in the approximation of the $\langle n(s) \rangle$ dependence by formula SM(1), CLM, LM(3). e^+e^- and pTa -collisions. Energy range ($2 \leq \sqrt{s} \leq 22$) GeV

e^+e^- -collisions

Formula	a	$b(\beta)$	c	χ^2/N
SM(1)	1.97±0.12	0.28±0.01		10/16
CLM(LM)(3)	3.33±0.55	-0.45±0.08	0.29±0.02	9/16

pp -collisions

SM(1)	1.21±0.07	0.32±0.01		3/14
CLM(LM)(3)	1.06±0.06	0.33±0.02	0.13±0.03	8/14

pTa – collisions

SM(1)	1.65±0.08	0.45±0.02		43/6
CLM(LM)(3)	-4.78±1.13	4.07±0.60	0.062±0.0124	3/6

CONCLUSIONS

1. The $\langle n(s) \rangle$ dependence on energy of the average multiplicity of charged secondary hadrons in e^+e^- - collisions is in principal well described by the statistical mode SM(1). The best description is obtained for high energy intervals ((10-200), (14-130), (10-130), (14-91)) GeV, when in each event more than six particles are produced (multiparticle

- events). The description of the $\langle n(s) \rangle$ dependence in the framework of the same model of pp -collisions is significantly worse. It is seen most well if the results in the same energy intervals are compared.
2. The Cluster (Lund) model and PQCD(4) describe data rather well but Cluster (Lund) model is more preferable.
 3. In the description of pp - collisions by formula (3) (CLM(LM)) as a rule the logarithmic term is more preferable, than in e^+e^- -collisions (in the same energy intervals) (Tables 2, 3, 6). This may be the reflection of the fact, that in pp -collisions the most part of secondaries is produced outside of jets.
 4. In e^+e^- - collisions the influence of the $\ln^2 s$ term (coefficient c) is more pronounced, than in pp and pTa – collisions. This may be the reflection of the fact, that the jet structure in e^+e^- - collisions is more pronounced, than in pp - and pTa -collisions.
 5. The fast growth of the average multiplicity in pTa -collisions is caused by the absorption of slow secondaries. Slower growth of the multiplicity above 10 GeV seems to be caused by the growth of the role of neutral particles in the total multiplicity.
 6. The Field-Feynman model describes well the data for e^+e^- - collisions only in high energy intervals.

REFERENCES

1. V.G. Grishin. Sov. J.Nucl. Phys. 1983, **38**, 967.
V.G. Grishin. Kvariki i adroni vo vzaemodeistviakh chastits vysokikh energii. M., 1988 (Russian).
R. D. Field, S. Wolfram. Nucl. Phys. B. 1983, **213**, 65.
2. V. S. Murzin and L. T. Saricheva. Vzaimodeistvia adronov visokikh energii. M., 1983 (Russian).
R. D. Field, R. P. Feynman. Nucl. Phys. B. 1980, **136**, 1.
3. Fujivara et al. Nucl. Phys. 1983, **A40**, 509.
4. P. Albrew et al. CERN-EP/2000-023, 7/2, 2000.

- Charged and identified particles in the hadronic decay. . . from (130-200) GeV (DELPHI Collaboration).
5. P. Albrecht et al. CERN-PPE/96-05, 22/1, 1996.
Charged particles multiplicity in e^+e^- -interactions at $\sqrt{s}=130$ GeV (DELPHI Collaboration).
 6. P. Albrecht et al. Z. Phys. C. (Particles and Fields) 1991, **50**, 185.
 7. P. Albrecht et al. Scaling violation in multiplicity distributions at 200 and 900 GeV; CERN-EP/85-197. 2/12, 1985.
 8. D. Brick et al. Phys. Rev. D. 1989, **39**, 2484.
 9. M. A. Dasaeva et al. Sov. J. Nucl. Phys., 1984, **39**, 846.
 10. N. S. Grigalashvili et al. Sov. J. Nucl. Phys., 1988, **48**, 476.
 11. E. N. Kladnitskaya. Fizika elementarnikh chastits i atomnogo iadra. 1982, **13**, 669.

Tbilisi State University

ლ. ახოზაძე, ვ. გარსევანიშვილი, ი. თევზაძე,
თ. ჯალაღანია, გ. ვანიშვილი

e^+e^- , pp - და pA_i -პროტონ-ბირთვის დაჯახებებში
დაბადებული მეორადი დამუხტული ადრონების საშუალო
მრავლობითობის ენერჯისაგან დამოკიდებულების
შედარებითი ანალიზი

დასკვნა

e^+e^- -ელექტრონ-პროტონის, pp -პროტონ-პროტონის (ანტი-
პროტონის), pA_i -პროტონ-ბირთვის დაჯახებებში დაბადებუ-
ლი მეორადი დამუხტული ადრონების $\langle n(s) \rangle$ -საშუალო
მრავლობითობის ენერჯისაგან დამოკიდებულების შედა-
რებითი ანალიზი, ჩატარებულია როგორც კლასიკური,
ასევე კვარკ-პარტონული მოდელების საფუძველზე.

ნაჩვენებია, რომ ექსპერიმენტს ყველაზე კარგად აღ-
წერს კლასტერული (ლუნდ) მოდელები. მაღალენერგეტი-
კულ არეში e^+e^- -დაჯახებებისათვის კარგად მუშაობს
სტატისტიკური მოდელი.